JOURNAL OF Applied Polymer SCIENCE

Simulation Study of the Morphologies of Energetic Block Copolymers Based on Glycidyl Azide Polymer

Zhou Yang,[1,2] Long Xin-Ping,[3] Zeng Qing-Xuan[2]

[1]Institute of Chemical Materials, Chinese Academy of Engineering and Physics, Mianyang 621900, China
[2]School of Mechanical and Electrical Engineering, Beijing Institute of Technology, Beijing 100081, China
[3]Chinese Academy of Engineering and Physics, Mianyang 621900, China
Correspondence to: Z. Yang (E-mail: zhouy@caep.ac.cn)

ABSTRACT: The morphologies of energetic block copolymers based on glycidyl azide polymer (GAP) were investigated by dissipative particle dynamics simulation. The results show that the morphologies could be used to qualitatively explain the variation in the mechanical properties of poly(azidomethyl ethylene oxide-*b*-butadiene) diblock copolymers (DBCs) and that bicontinuous (B) phases could effectively improve the mechanical properties. Among our designed DBCs, only GAP–acrylic acid, GAP–acrylonitrile, and GAP–vinyl amide could form B phases at very narrow regions of GAP contents. The triblock copolymers with their linear topologies could maintain the B phases in the broader region of GAP contents. We hope these results can provide help in the design and synthesis of new energetic block copolymers. © 2012 Wiley Periodicals, Inc. J. Appl. Polym. Sci. 129: 480–486, 2013

KEYWORDS: copolymers; morphology; theory and modeling

Received 31 May 2012; accepted 16 August 2012; published online 22 November 2012
DOI: 10.1002/app.38482

INTRODUCTION

Because of intrinsic limitations, many conventional propellants have become a major source of pollution when space vehicles or missiles are launched; this has significant impacts for their development. For example, AP-based propellants can result in the exhaust of 220 tons of hydrochloride and tremendous environmental pollution hazards from a single launch of the U.S. space shuttle.[1] Therefore, the search for new propellants that have a higher impulse, higher control of burning rate, higher safety and reliability, and no or lower pollution is still a challenging task. New energetic polymers have become one of the promising materials that could satisfy these requirements. Among them, glycidyl azide polymer (GAP) is one of the most thoroughly studied energetic binders; its synthesis, performance, and applications have been reported in detail by several researchers.[2–9] Although GAP has many major advantages, such as a higher energy output, higher density, and good compatibility with high-energetic oxidizers such as ammonium dinitramide and hydrazinium nitroformate (HNF),[10] the low-temperature properties of GAP are poor because of its low weight percentage of polymer weight-bearing chains. The critical temperature (6°C) and glass-transition temperature (−43°C) of GAP are far greater than those of hydroxyl-terminated polybutadiene (HTPB), and this significantly restricts its application in solid propellants.[11] It is a natural idea that we could improve this by the design of blends or copolymers.[5,7,9] On the basis of the dissipative particle dynamics (DPD) method, we studied the interfacial tension (γ) of incompatible GAP/HTPB blends in the presence of block copolymers and plasticizers.[12] The results show that copolymers and plasticizers in the propellants could effectively improve the γ of GAP/HTPB blends and increase their compatibility. In this study, we continued to examine energetic copolymers by the same method. For energetic copolymers, studies have focused mainly on the synthesis and characterization and have rarely focused on the relationship between their structures and properties. This relationship is important in the design of new energetic block copolymers with better properties.

The properties of energetic block copolymers (especially the mechanical properties) depend not only on their molecular structures but also on their morphologies. Therefore, we investigated the morphologies of block copolymers based on the energetic binder GAP. In fact, several empirical or semiempirical methods can calculate the mechanical properties on the basis of the chemical composition and molecular structure for copolymer systems, such as the relationships (adapted to small-strain behavior, i.e., small deformations) developed by Seitz,[13] which obviously ignore the effect of the morphology of copolymer systems.[14] It is the morphology (5–100 nm) from the microphase separation that can significantly influence the mechanical properties of block copolymer materials.[15–18] To understand the

influence of their structures on the properties of energetic block copolymers, we need information on their morphologies and to take them as a bridge linking the microstructures and the macroproperties. The main aim of this work was to construct the relationship between the morphologies and molecular structures of energetic block copolymers from the bottom up. In addition, experimental studies are very expensive and dangerous for energetic materials; this made DPD a good choice for studying this problem. Moreover, computer simulations, especially DPD simulation, are capable of providing valuable mesoscopic morphologies of the actual polymer systems.[19–22] In this study, by means of DPD simulation, we provided the first detailed mesoscale understanding of the morphology of energetic block copolymers based on GAP. We were concerned about three key parameters: the Flory–Huggins interaction parameter (χ), the chain length (N) of the copolymer, and the volume fraction (f) of the energetic blocks.

SIMULATION DETAILS

The DPD method is a coarse-grained particle-based dynamics simulation technique that can correctly describe hydrodynamics behavior.[23,24] The interaction between DPD particles can be expressed by a conservative force (F^C), a dissipative force (F^D), and a random force (F^R). The total force exerted on particle i (f_i) is given by

$$f_i = \sum_{j \neq i} [F_{ij}^C + F_{ij}^D + F_{ij}^R] \tag{1}$$

The different parts of the three forces describing the nonbonded interaction are given by

$$\begin{aligned} F_{ij}^C &= -a_{ij} w^C(r_{ij}) e_{ij} \\ F_{ij}^D &= -\gamma w^D(r_{ij})(e_{ij} v_{ij}) e_{ij} \\ F_{ij}^R &= \sigma w^R(r_{ij}) \xi_{ij} \Delta t^{-0.5} e_{ij} \end{aligned} \tag{2}$$

where y and σ are defined as the friction coefficient and the amplitude of the noise; $r_{ij} = r_i - r_j$, $r_{ij} = |r_{ij}|$, $e_{ij} = r_{ij}/r_{ij}$, and $v_{ij} = v_i - v_j$; ξ_{ij} is a random number with zero mean and unit variance; α_{ij} is the maximum repulsion, which reflects the chemical characteristics of interacting particles; and w^C, w^D, and w^R are three weight functions. For w^C, simple forms are chosen as follows: $w^C(r_{ij}) = 1 - r_{ij}$ for $r_{ij} < 1$ and $w^C(r_{ij}) = 0$ for $r_{ij} \geq 1$.[25] Unlike w^C, w^D and w^R have a certain relationship to satisfy the fluctuation–dissipation theorem

$$\begin{aligned} w^D(r_{ij}) &= [w^R(r_{ij})]^2 \\ \sigma^2 &= 2\gamma k_B T \end{aligned} \tag{3}$$

where w^D and w^R also use the simple form as same as w^C. In addition, the forces describing the connected particles $[F_{(i,i+1)}^S]$ are obtained by the differential of the spring potential:

$$F_{(i,i+1)}^S = -\nabla U_{(i,i+1)}^S \text{and} U_{(i,i+1)}^S = \sum_i 1/2 k_S [l_{(i,i+1)} - l_0]^2 \tag{4}$$

where $l_{(i,i+1)}$ is the bond length between the two connected particles i and $i+1$, l_0 is the equilibrium bond length and K_s is the spring constant. In DPD, the particles connected by the spring force can be used to represent the polymer. The simulations are performed with the DPD program of Materials Studio software (Accelrys, San Diego, USA), and we chose the radius of interaction (r_c), particle mass (m), and temperature (T) as $r_c = m = k_B T = 1$, where k_B is Boltzmann constant. The repulsion parameter (a_{ij}) between DPD particles can be mapped with Flory–Huggins theory through the relation $a_{ij} = a_{ii} + 3.27\chi$ ($\rho = 3$), where a_{ii} has a value of $25 k_B T$, which gives a pure DPD fluid with a compressibility similar to that of liquid water.[25]

The same model and parameters from our study on the interfaces of the GAP/HTPB blends[12] were used for the energetic copolymer GAP–HTPB; the details of the coarse-grained model and parameters calculation are not introduced again. In addition, to find copolymers with better morphologies, a series of energetic block copolymers based on GAP were designed. To

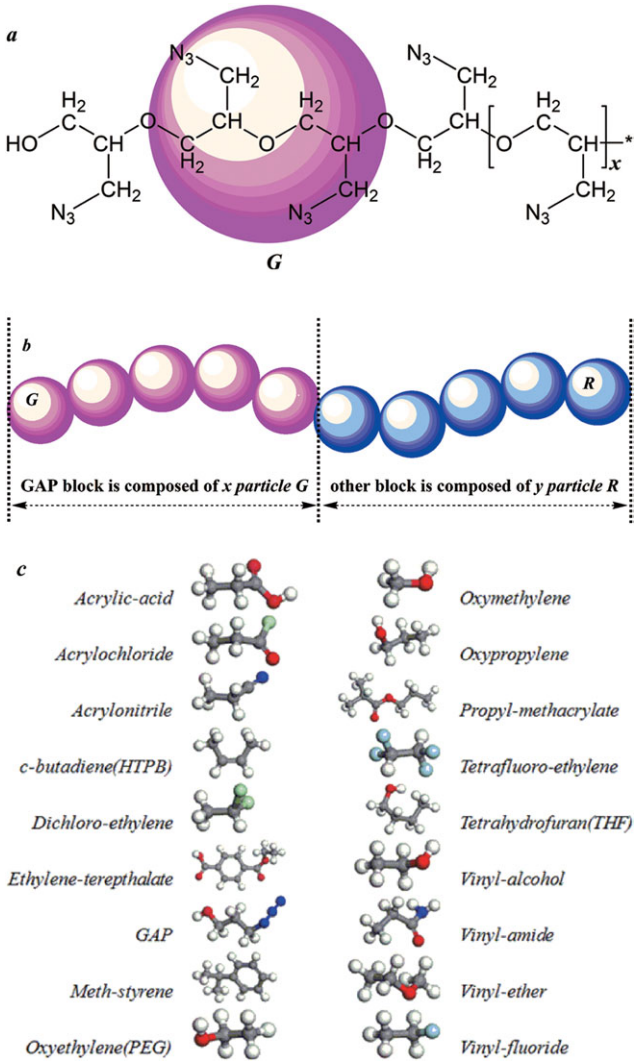

Figure 1. Coarse-grained model for the energetic block copolymer based on GAP: (a) molecular structure of GAP, (b) coarse-grained model for the energetic copolymer, and (c) repeat units for the other block. [Color figure can be viewed in the online issue, which is available at wileyonlinelibrary.com.]

Table I. Comparison of the Computed and Experimental Solubility Parameters

	δ_{exp}[a]	δ_{Fedors}	δ_{van}	δ
GAP	22.5	20.9	21.2	21.05
HTPB	16.6-17.6	17.4	17.7	17.55
PCL	21.0	20.6	18.0	19.3
PEG	20.0	18.3	19.1	18.7

PCL, polycaprolactone; PEG, polyoxyethylene.
[a]Data from Refs. 28 and 29.

reduce the calculation, a larger, coarse-grained model was used, in which several repeat units of GAP were lumped together into a DPD particle [G; see Figure 1(a)]. χ was obtained by the equation $\chi = V_{bead}(\delta_i - \delta_j)^2/kT$,[27] where δ_i and δ_j are the solubility parameters of the pure component and V_{bead} is the volume of a DPD particle. Then, we could obtain other coarse-grain blocks based on particle G with the same volume in DPD [see Figure 1(b,c)]. Reliable average values of δ for long-chain polymers could be estimated from simple correlation methods. The results are listed in Tables I and II. Table I gives the results of the comparison between the computed and experimental δ parameters for several familiar segments in the energetic block copolymers, where δ is an average of the Fedors and van Krevelen solubility parameters (δ_{Fedors} and δ_{van}, respectively) obtained from the SYNTHIA code (Accelrys). The results show that the δ parameters calculated by the SYNTHIA code were in good agreement with the experimental results.

Through the root mean square end-to-end distance of the longest copolymers having no obvious variation with increasing box length, we judged that the selected box could effectively eliminate the finite size effect. Therefore, a cubic simulation box of 40^3 with a periodic boundary condition of three directions was applied. A time step of 0.05 was used, and a total of 1–3 $\times$ 10^6 DPD steps were carried out for the DPD simulations.

RESULTS AND DISCUSSION

Diblock Copolymer (DBC) Systems

The fine control of morphologies is very important for tailoring the basic mechanical properties of such copolymer systems. First, the morphologies of DBC GAP-*b*-HTPB were investigated,

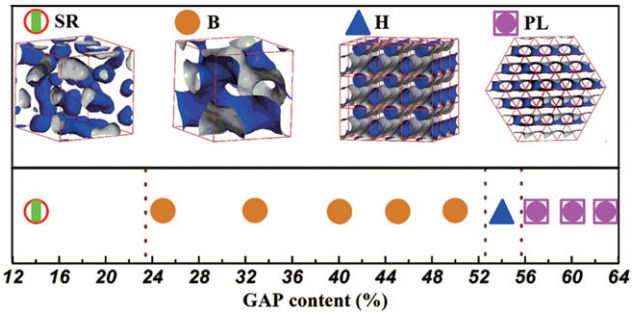

Figure 2. Relation between the morphology and GAP content for GAP-*b*-HTPB. The outward surfaces of the GAP phases are colored blue in the online figure, and the rest are HTPB phases. [Color figure can be viewed in the online issue, which is available at wileyonlinelibrary.com.]

and the results are drawn in Figure 2. Figure 2 shows that when the contents of the energetic block GAP were less than 52 wt %, GAP-*b*-HTPB formed morphologies in which HTPB was the continuous phase and GAP was the disperse phase; this mainly included a random mix of spheres (Hs) and the liquid rod (SR) phase, the bicontinuous (B) phase. When the GAP content was greater than 52 wt %, GAP-*b*-HTPB showed inversed phases in which GAP became the continuous phase and HTPB was the disperse phase, which had hexagonal cylindrical (H) and perforated lamellae (PL) phases. B morphologies are of special interest for interconnectivity in all three directions, which not only gives them unusual mechanical properties but also makes them perfect candidates as precursors of porous materials, catalytic surfaces, and high-conductivity nanocomposites.[30,31] In general, B structures include the gyroid (G), the double diamond (DD), the plumber's nightmare (P), and the Neovius phases.[32,33] However, the G phase was the only stable B morphology for the pure DBC system.[34] Recent studies have also predicted[35,36] and observed[37] the orthorhombic *Fddd* (O)[70] network phase. Our studied GAP-*b*-HTPB copolymer is a common DBC, and the morphology should be the stable G phase. To ensure that the morphology actually corresponded to the G phase, the structure factor [$S(q)$] was calculated by the Fourier transition of radial distribution functions [$g(r)$'s]. The results of $S(q)$ and $g(r)$ are shown in Figure 3. For $g(r)$, the GAP-*b*-HTPB copolymers had a similar distribution when their morphologies belonged to the range of B phase (see Figure 2). Therefore, we only calculated

Table II. Interaction Parameters for the Designed GAP Copolymers

i–*j*	χN	*i*–*j*	χN
GAP–methstyrene	8.0	GAP–THF	27.0
GAP–propyl methacrylate	8.2	GAP–difluoroethylene	30.1
GAP–ethylene terepthalate	8.6	GAP–vinyl ether	30.5
GAP–dichloroethylene	11.3	GAP–oxypropylene	32.0
GAP–oxymethylene	14.6	GAP–acrylic acid	37.2
GAP–acrylochloride	17.8	GAP–acrylonitrile	48.2
GAP–oxyethylene	22.6	GAP–vinyl amide	52.2
GAP–vinyl fluoride	23.8	GAP–vinyl alcohol	79.1

THF, tetrahydrofuran.

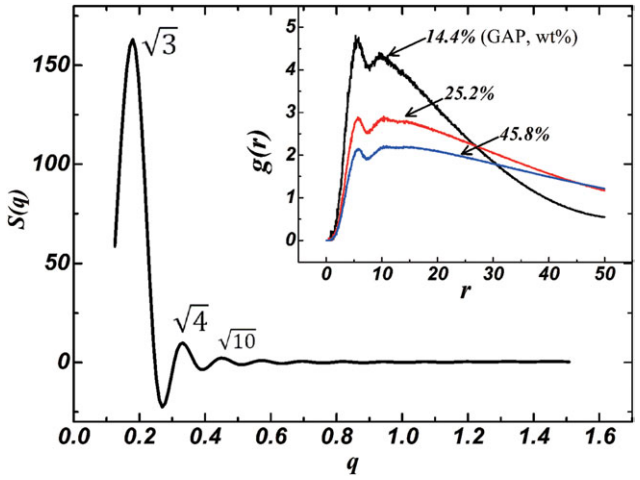

Figure 3. $S(q)$ calculated from a simulated snapshot of the B phase, q is the spatial frequency. The inset shows $g(r)$ for the different GAP contents. [Color figure can be viewed in the online issue, which is available at wileyonlinelibrary.com.]

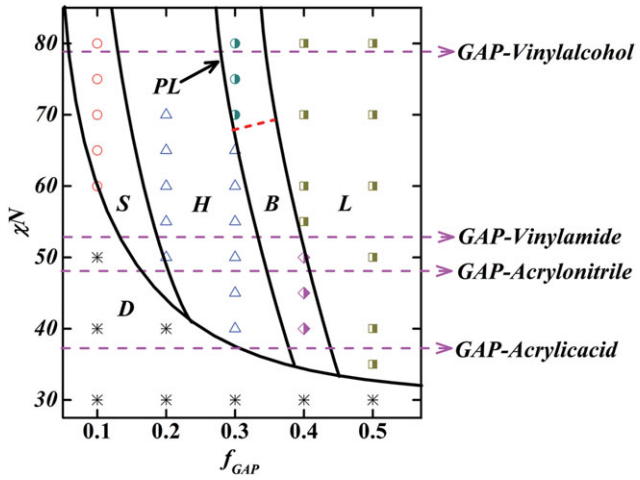

Figure 5. Simulated phase diagram for the DBCs (χN vs f). Regions of totally disordered (D), L, PL, Hs, S, and B phases are shown. The boundary lines were drawn to guide the eye. [Color figure can be viewed in the online issue, which is available at wileyonlinelibrary.com.]

one $S(q)$ for the GAP-*b*-HTPB copolymer with a GAP of 45.8%. A comparison of the location of the first three peaks showed good agreement with the ratios that were observed theoretically[38] (i.e., $\sqrt{3} : \sqrt{4} : \sqrt{10}$); this provided evidence for the formation of the G phase. However, we still used the B phase as a tag in Figure 2 because we confirmed that other B morphologies could give the same unusual mechanical properties as the G phase. In fact, B structures have a three-dimensional periodicity and thus depend on the simulation box size. If the simulation box size is changed, the final morphology may be others, such as DD, P, or O[70], not G. It certainly does not distract from our point that B phases (including G, O[70], or other phases) provide good mechanical properties. Therefore, we did not investigate the effects of the different simulation box sizes.

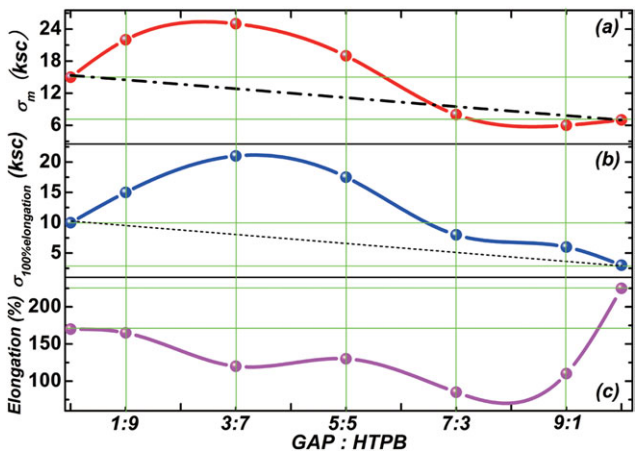

Figure 4. Relation between the mechanical properties [(a) tensile strength, (b) stress at 100% elongation ($\sigma_{100\%elongation}$), and (c) σ_m] and the GAP content for GAP-*b*-HTPB. The figure was drawn by us on basis of the experimental results.[38] [Color figure can be viewed in the online issue, which is available at wileyonlinelibrary.com.]

To construct a link between the morphology and the macroproperties, we summarized the experimental data of the mechanical properties for GAP-*b*-HTPB,[38] where the energetic block copolymers were synthesized by the curing reaction. The results are given in Figure 4. Then, we tried to qualitatively analyze the effects of the morphologies on the mechanical properties. From Figure 4(a), we can clearly see that the tensile strength of the pure HTPB was greater than that of pure GAP. If the morphology had no influence on the mechanical properties, the tensile strength of the block copolymer GAP-*b*-HTPB should have dropped along the straight line with increasing GAP content. In fact, this copolymer showed better tensile strength and stress at 100% elongation values than the pure HTPB in the range of about 30–50 wt % GAP. Figure 2 shows clearly that in this range, the morphologies of energetic DBC GAP-*b*-HTPB were composed of the continuous phase of HTPB and the disperse phase of GAP. Moreover, the calculations of SYNTHIA code (Accelrys) showed that the Young's (or shear) modulus of HTPB with the facile chain was far lower than that of GAP with the larger side chain. Therefore, we owed the improved mechanical properties of GAP-*b*-HTPB in the range of 30–50% to the reinforcement effect of the GAP phase, especially the formation of the B phase. Once the GAP content exceeded about

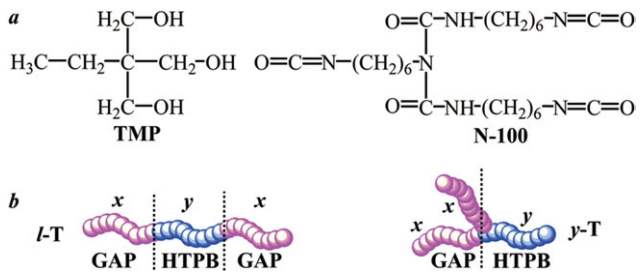

Figure 6. (a) Molecular structures of the polyfunctional reactants TMP and N-100 and (b) topological structures of the triblock copolymers (pink block = GAP, blue block = HTPB). [Color figure can be viewed in the online issue, which is available at wileyonlinelibrary.com.]

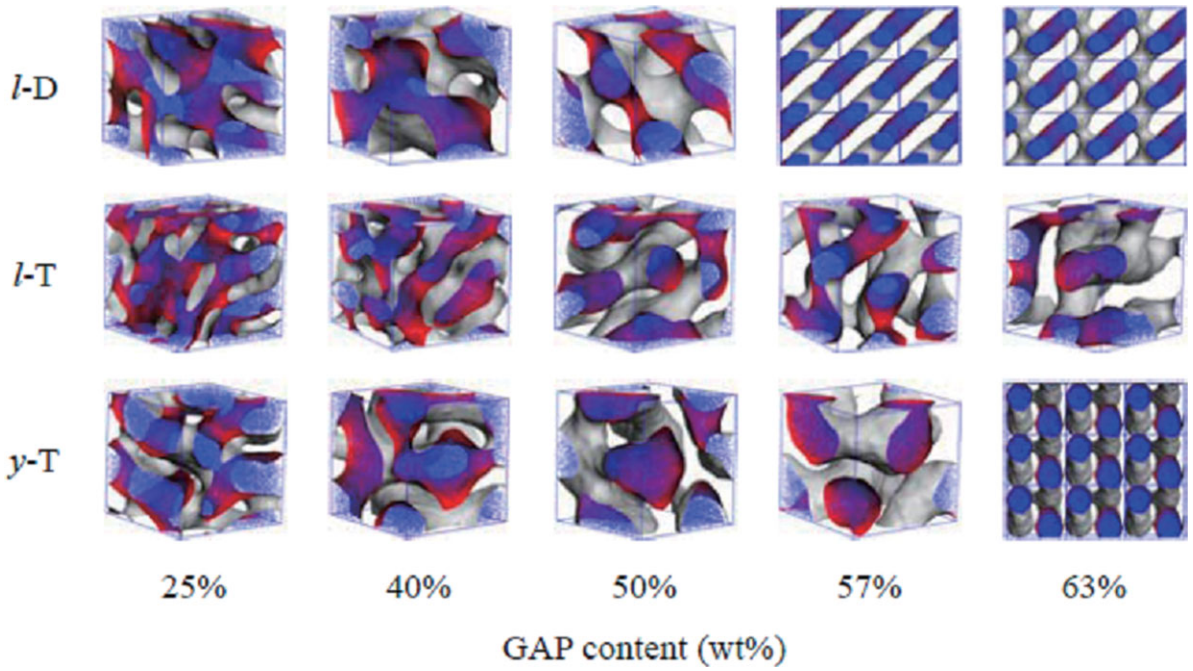

Figure 7. Morphologies for *l*-D, *l*-T, and *y*-T complicated block GAP/HTPB copolymers. The outward surfaces of the GAP phases are red, and the rest are the HTPB phases (blue). [Color figure can be viewed in the online issue, which is available at wileyonlinelibrary.com.]

50%, the tensile strength and stress at 100% elongation of GAP-*b*-HTPB appeared as distinct declines. At one time, in the morphology of GAP-*b*-HTPB arose the reverse, that is, GAP formed the continuous phase, and HTPB became the disperse phase. The experiment results testified that the reinforcement effect of HTPB was far less than that of GAP. A possible reason was that GAP had a larger modulus than HTPB. Moreover, GAP-*b*-HTPB, as shown in Figure 2, formed the PL phase when the GAP content was greater than 56%. In studies of poly(styrene-*b*-*n*-butylmethacrylate) DBCs, Weidisch and coworkers[15,16] found that the formation of the lamellar (L) structure was responsible for the degradation in mechanical properties. In addition, they believed that the B phase was one reason for the improved mechanical properties. These results were in good agreement with our findings on the GAP-*b*-HTPB DBCs. Figure 4(c) also shows that the elongation of HTPB was better than that of GAP; this could attributed to the facile main chain of HTPB and the larger side chain of GAP. As a whole, the experimental result testified that the elongation properties of GAP-*b*-HTPB declined and were even lower than those of GAP. There were comparatively good elongation properties when the GAP content was about 50%; this also corresponded to the B phase. If we ignored the error between the simulation and the experiment, we might also believe that the result was in good agreement with the viewpoint of Weidisch and coworkers. From the previous discussion, we could qualitatively link the evolvement of diblock GAP-*b*-HTPB morphologies with its macromechanical properties. The main finding was that the B phase could effectively improve the mechanical properties of energetic DBC GAP-*b*-HTPB.

To provide more energetic block copolymers with good mechanical properties as candidates, we designed a series of diblock GAP copolymers. One block of these copolymers was GAP. Sixteen homopolymers were selected one by one as other blocks, and their repeat units are drawn in Figure 1(c). Because of the expense of the calculation, a new coarse-grained tactic [Figure 1(b)] was used, and χN ($N = 20$) was computed. The values are listed in Table II. To obtain a whole-phase diagram, we added several interaction parameters that are not listed in Table II. Then, our simulation parameter space was expanded to different composition fractions: $f_{GAP} = x/(x + y)$ x, y is the number of particle G and R, respectively [see Figure 1(b)]. Figure 5 presents a simple phase diagram, which does not distinguish between the body-centered-cubic (bcc) and face-centered-cubic (fcc) spherical, gyroid, and O^{70} morphologies, by our DPD simulation. However, the regional distributions of the main phases (D, S, H, L, etc.) were in agreement with a prediction by Matsen.[36] In addition, between the H phase and the L phase, we found a PL phase. This phase was not predicted from self-consistent field theory (SCFT), but Groot and Madden[20] also found it at $f = 0.325$ and 0.35 by DPD simulation. In fact, because we did not investigate the simulation box size, it is possible that the PL and gyroid phases were not distinct but rather that the PL phase was metastable relative to the gyroid phase. The difference of this region did not influence our conclusions because we were only concerned with the region of the B (gyroid or O^{70}) phase. As shown in Figure 5 and other predicted phase diagrams, there were narrow regions of B phase but wider regions that could form L (PL or L) structures. Therefore, it was not an easy task to search for an appropriate GAP copolymer with good mechanical properties. When the total degree of polymerization was fixed ($N = 20$), only three energetic DBCs, GAP–acrylic acid, GAP–acrylonitrile, and GAP–vinyl amide, came through the narrow region of B phase with increasing GAP content; this provided evidence that they

could form the B phase. As mentioned previously, the B phase could effectively improve the mechanical properties.

Triblock Copolymer Systems

In fact, DBCs are difficult to obtain in real experiments because of their complicated reaction condition. However, linear triblock (*l*-T)[9,12] or *y*-type triblock (*y*-T) copolymers are often synthesized, especially when the reaction systems contain polyfunctional reactants such as trimethylol propane (TMP) or Desmodur N-100 polyisocyanate (their molecular and topological structures are plotted in Figure 6). Therefore, we studied the effect of topological structures on the morphologies of the GAP/HTPB triblock copolymers. In fact, there may be many other energetic triblock copolymers that could also be synthesized experimentally. Here, we still used GAP/HTPB triblock copolymers as example for convenient comparison with the previous linear diblock (*l*-D) copolymers.

For the *l*-T and *y*-T GAP/HTPB copolymers, the same coarse-grained model with the *l*-D copolymer GAP-*b*-HTPB was again used to investigate their morphologies. The results are given in Figure 7, which shows that the *l*-D, *l*-T, and *y*-T copolymers could form the B phase, which could provide good mechanical properties when the weight content of GAP was 25 or 40%. When GAP content increased from 40 to 50%, only the linear copolymers (*l*-D and *l*-T) could retain the B morphologies. The copolymer *y*-T showed an uncontinuous morphology, which was a small quantity of the SR phase of HTPB dispersed in the continuous GAP phase. When GAP content was equal to 57%, the *l*-D copolymer formed the PL phase, and the *y*-T copolymer showed a more complete uncontinuous morphology, in which all of the HTPB components became the dispersed phase. Only the *l*-D copolymer retained the B morphology, even though the GAP content was 63%. For this level of GAP content, the *y*-T copolymer became the H structures; that is, the H HTPB phases dispersed in the continuous GAP phase, and the *l*-D copolymer still retained the PL phase. On the basis of the previous analysis, *l*-T copolymers could theoretically provide better mechanical properties while ensuring a higher GAP content. GAP is the energetic binder, but HTPB is not. Therefore, a higher GAP content in solid propellants could provide more energy output; this is very important for space vehicles and missiles.

CONCLUSIONS

In this study, DPD simulation methods were first used to investigate the morphologies of energetic block copolymer systems based on energetic GAP. We mainly studied the influence of molecular formation on the morphology of the energetic block copolymer systems by changing the GAP contents, different blocks, and topological structures.

First, for GAP-*b*-HTPB DBC, we simply analyzed the effect of the morphologies on the mechanical properties on the basis of experimental results.[15,16,38] Through comparisons of our simulated morphologies and mechanical properties, we observed that the so-called B phase had an obvious advantage in improving the mechanical properties. However, in the phase diagram for our designed GAP DBCs, the results show that the range of energetic GAP copolymers that could form the B phase was very narrow. Among the 16 homopolymers selected by us, only three were in this range. Second, for the GAP/HTPB triblock copolymers, we found that GAP/HTPB triblock copolymers with the linear topology (*l*-T) could maintain the B phase in a broader region of GAP contents. However, the *y*-T topology could lose the B phase, and the uncontinuous phase appeared only when the GAP content exceeded 50 wt %. We hope that these results can help experimental researchers select appropriate materials in the design and synthesis of new energetic block copolymers for bulky space components, when these energetic block copolymers are used as the binders of solid propellants, and that they can provide better macroscale properties and decrease pollution.

Finally, we have to emphasize that because we did not investigate the simulation box size, several changes may have, in fact, been related to changing periodicity as the building block was changed. However, this does not take away from the importance of our conclusions. The previous analysis in Figure 5 clearly shows that new simulations for the phase diagram need not to be performed, and experimentalists can reasonably rely on prior work to aid in the design of new energetic binders of solid propellants.

ACKNOWLEDGMENT

The authors appreciate the financial support from the Foundation of Chinese Academy of Engineering and Physics (contract grant numbers 2012B0302037, 2011A0302014, and 2010A03002) and the National Nature Sciences Foundation of China (contract grant numbers 51173173 and 21173199). The authors are also grateful to the editors and reviewers for their effective work.

REFERENCES

1. Nazare, N.; Asthana, S. N.; Singh, H. *J. Energy Mater.* **1992**, *10*, 43.
2. Mohan, Y. M.; Raju, M. P.; Raju, K. M. *J. Appl. Polym. Sci.* **2004**, *93*, 2157.
3. Manu, S. K.; Sekkar, V.; Scariah, K. J.; Varghese, T. L.; Mathew, S. *J. Appl. Polym. Sci.* **2008**, *110*, 908.
4. Mathew, S.; Manu, S. K.; Varghese, T. L. *Propell. Explos. Pyrotech.* **2008**, *33*, 146.
5. Mohan, Y. M.; Raju, K. M. *Int. J. Polym. Mater.* **2006**, *55*, 203.
6. Vasudevan, V.; Sundararajan, G. *Propell. Explos. Pyrotech.* **1999**, *24*, 295.
7. Abou-Rachid, H.; Lussier, L. S.; Ringuette, S.; Lafleur, L. X.; Jaidann, M.; Brisson, J. *Propell. Explos. Pyrotech.* **2008**, *33*, 301.
8. Manu, S. K.; Varghese, T. L.; Mathew, S.; Ninan, K. N. *J. Propul. Power* **2009**, *25*, 533.
9. Subramanian, K. *Eur. Polym. J.* **1999**, *35*, 1403.
10. Mohan, Y. M.; Mani, Y.; Raju, K. M. *Des. Monomers Polym.* **2006**, *9*, 201.
11. Mohan, Y. M.; Raju, K. M. *Des. Monomers Polym.* **2005**, *8*, 159.
12. Zhou, Y.; Long, X. P.; Zeng, Q. X. *J. Appl. Polym. Sci.* **2012**, *125*, 1530.

13. Seitz, J. T. *J. Appl. Polym. Sci.* **1993**, *49*, 1331.
14. Soto-Figueroa, C.; Rodriguez-Hidalgo, M. R.; Martinez-Magadanb, J. M. *Polymer* **2005**, *46*, 7485.
15. Weidisch, R.; Michler, G. H.; Fischer, H.; Arnold, M.; Hofmann, S.; Stamm, M. *Polymer* **1999**, *40*, 1191.
16. Weidisch, R.; Michler, G. H.; Arnold, M. *Polymer* **2000**, *41*, 2231.
17. Weidisch, R.; Stamm, M.; Michler, G. H.; Fischer, H. *Macromolecules* **1999**, *32*, 5375.
18. Weidisch, R.; Ensslen, M.; Michler, G. H.; Stamm, M.; Schubert, D. W.; Budde, H.; Horing, S.; Arnold, M.; Jerome, R. *Macromolecules* **2000**, *33*, 5495.
19. Soto-Figueroa, C.; Vicente, L.; Martinez-Magadanb, J. M.; Rodriguez, M. R. *Polymer* **2007**, *48*, 3902.
20. Groot, R. D.; Madden, T. J. *J. Chem. Phys.* **1998**, *108*, 8713.
21. Martinez-Veracoechea, F. J.; Escobedo, F. A. *J. Chem. Phys.* **2006**, *125*, 104907.
22. Qian, H. J.; Lu, Z. Y.; Chen, L. J.; Li, Z. S.; Sun, C. C. *Macromolecules* **2005**, *38*, 1395.
23. Hoogerbrugge, P. J.; Koelman, J. M. V. *Europhys. Lett.* **1992**, *19*, 155.
24. Espanol, P.; Warren, P. B. *Europhys. Lett.* **1995**, *30*, 191.
25. Groot, R. D.; Warren, P. B. *J. Chem. Phys.* **1997**, *107*, 4423.
26. Stacer, R. G.; Husband, D. M. *Propell. Explos. Pyrotech.* **1991**, *16*, 167.
27. Maiti, A.; McGrother, S. *J. Chem. Phys.* **2004**, *120*, 1594.
28. Min, B. S. *Macromol. Res.* **2007**, *15*, 225.
29. Brabdrup, J.; Immergut, E. H.; Grulke, E. A. Polymer Handbook; Wiley: New York, **1999**.
30. Kamperman, M.; Garcia, C. B. W.; Du, P.; Ow, H.; Wiesner, U. *J. Am. Chem. Soc.* **2004**, *126*, 14708.
31. Cho, B.-K.; Jain, A.; Gruner, S. M.; Wiesner, U. *Science* **2004**, *305*, 1598.
32. Strom, P.; Anderson, D. M. *Langmuir* **1992**, *8*, 691.
33. Martinez-Veracoechea, F. J.; Escobedo, F. A. *Macromolecules* **2009**, *42*, 9058.
34. Matsen, M. W.; Schick, M. *Phys. Rev. Lett.* **1994**, *72*, 2660.
35. Guo, Z. J.; Zhang, G. J.; Qiu, F.; Zhang, H. D.; Yang, Y. L.; Shi, A. C. *Phys. Rev. Lett.* **2008**, *101*, 4.
36. Matsen, M. W. *Macromolecules* **2012**, *45*, 2161.
37. Kim, M. I.; Wakada, T.; Akasaka, S.; Nishitsuji, S.; Saijo, K.; Hasegawa, H.; Ito, K.; Takenaka, M. *Macromolecules* **2008**, *41*, 7667.
38. Manu, S. K.; Varghese, T. L.; Joseph, M. A.; Shanmugam, K.; Mathew, S. In Proceedings of the 35th International Annual Conference, Institute of Chemical Technology, Karlsruhe, Germany, **2004**; p 1/98.